Energy Engineering

Tech Science Press

DOI: 10.32604/ee.2022.022759

ARTICLE

Hydroprocessing and Blending of a Biomass-Based DTG-Gasoline

David Graf, Philipp Neuner and Reinhard Rauch*

Department Fuel Technology (EBI-ceb), Karlsruhe Institute of Technology (KIT), Engler-Bunte-Institute, Karlsruhe, 76131, Germany

*Corresponding Author: Reinhard Rauch. Email: Reinhard.Rauch@kit.edu

Received: 24 March 2022 Accepted: 26 May 2022

ABSTRACT

The number of annually registered internal-combustion vehicles still exceeds electric-driven ones in most regions, e.g., Germany. Ambitious goals are disclosed with the European Green Deal, which calls for new technical approaches and greenhouse gas neutral transition technologies. Such bridging technologies are synthetic fuels for the transportation sector, e.g., using the bioliq® process for a CO_2-neutral gasoline supply. Fuels must meet the applicable national standards to be used in existing engines. Petrochemical parameters can be variably adapted to their requirements by hydroprocessing. In this work, we considered the upgrading of aromatic-rich DTG gasoline from the bioliq® process. The heavy gasoline was therefore separated from the light one by rectification. We investigated how to selectively modify the petrochemical parameters of the heavy gasoline, especially the boiling characteristics, to make the product suitable as a high-quality blending component. Three commercially available Pt/zeolite catalysts were tested over a wide range of temperature and space velocity. We achieved high gasoline yields, while the content of light end compounds up to a boiling temperature of 150°C could be increased significantly. In contrast to the high naphthenic content of the gasoline, the obtained octane numbers were satisfactory. Especially the Motor Octane Number turned out unexpectedly high and showed a dependency on the isomerization of the naphthenic rings. By blending the upgraded heavy gasoline with the previously separated light gasoline, we could finally show that hydroprocessing is suitable for adjusting petrochemical parameters. The aromatic concentration was 37.5% lower than that in the original raw gasoline, while the boiling characteristics improved significantly. Additionally, the final boiling point was 82°C lower, which is beneficial for the emission behavior.

KEYWORDS

Synthetic fuels; upgrading; durene; dimethyl ether to gasoline; refinery

Abbreviations

ASTM	American society for testing and materials
CFR	Cooperative fuel research
DIN	German industry standard
DMCP	Dimethylcyclopentane
DME	Dimethyl ether
DTG	Dimethyl ether to gasoline
ECP	Ethylcyclopentane
EN	European standard

FT	Fischer-Tropsch synthesis
FTIR	Fourier-transform infrared
GC	Gas chromatograph
GHG	Greenhouse gas
HP	Hydroprocessing
ISO	International organization for standardization
MCH	Methylcyclohexane
MFC	Mass flow controller
MTG	Methanol to gasoline
RC	Ring contraction
RO	Ring opening

Nomenclature

$E70$	Evaporated volume at 70°C
FBP	Final boiling point
H_R^0	Standard enthalpy of reaction
m	Mass
MON	Motor octane number
p_v	Vapor pressure
φ	Volume fraction
ρ	Density
RON	Research octane number
T	Reaction temperature
t_R	Reaction time
V	Volume
w	Mass fraction
$WHSV$	Weight hourly space velocity
x	Mole fraction
$Y_{Gasoline}$	Mass yield of gasoline

1 Introduction

As the greatest challenge of the present, the global climate crisis has underlined the urgency of a rapid expansion of renewable energies and the associated reduction of greenhouse gas (GHG) emissions. Many countries are starting to transform their energy sector towards greater sustainability, including the European Union with the Green Deal [1]. The transformation aims to comprehensively create a CO_2-neutral economy and society by 2050, which focuses on the sustainable use of available raw materials while preserving biodiversity [2]. This concept addresses all sectors of the energy system, of which the transport sector accounts for a significant share of total GHG emissions, e.g., 20% in Germany [3].

Automobiles based on electric drives are considered the most promising technology for decarbonizing the traffic sector in the medium to long term. According to official numbers of the German Federal Motor Transport Authority, the rate of new registered electric-driven cars increased in 2021 by 83.3% [4]. However, the share of car sales with internal-combustion engines still exceeds those of electric-driven ones. Newly registered vehicles counted 13.6% for fully electric drives and 12.4% for hybrid ones on German roads. Moreover, the average age of a car in Germany is approx. ten years, and

the number older than 30 years has increased by 15% (Jan 2022) [5]. Therefore, the ambitious climate targets can only be achieved if a GHG neutral alternative can be provided for the transition period of vehicles that still rely on an internal-combustion engine. A more distinct situation is emerging for the heavy transportation and aviation sectors, as they are strongly dependent on energy sources with high energy densities. These sectors are expected to depend on liquid hydrocarbon fuels in the long term. Due to these circumstances, it is important to continue investigating synthetic fuels as potential alternatives.

Feedstocks will become increasingly variable in the coming decades. Refineries will have to deal with biological feedstocks besides heavier fossil ones like tar sand [6]. Fischer-Tropsch (FT) and methanol to gasoline (MTG) or dimethyl ether to gasoline (DTG) are well known for decades. They can be considered part of the backbone for multifaceted hydrocarbon supply in the future. In contrast to process development and optimization, practical integration into refineries and the associated challenges have not been discussed in great detail. Processes such as FT and MTG or DTG place new demands on fuel upgrading. Due to the high concentration of aromatics, synthetic MTG and DTG gasolines differ considerably from fossil ones. Especially 1,2,4,5-Tetramethylbenzene (durene) can cause drivability problems. Crystallization resulting from the low melting temperature of 79°C can consequently clog fuel injection systems [7].

In refineries, several upgrading strategies are available or can be integrated, which are: a) transalkylation/disproportionation, b) extraction/crystallization, c) dilution and d) upgrading by hydroprocessing (HP). Processes for transalkylation and disproportionation have already been commercialized, for example with the Mobil TransPlus^{SM} process, which converts heavy aromatics into valuable BTX aromatics [8]. However, transalkylation is not available in every refinery. Due to increased process requirements resulting from the high reaction temperatures and thermodynamically limited conversion rates, significant investment costs must be considered. Crystallization or extraction of durene is promising as it opens synthesis routes with durene as a basic chemical, e.g., the production of polyimides [9]. However, this might only be a long-term solution, as new processes and infrastructures are required. Without major investment, the durene could be diluted into other hydrocarbon streams in the refinery by implementing a metering unit. Laboratory tests showed satisfactory engine performances with durene concentrations up to 5 wt.% [7,10,11]. However, heavy aromatics tend to form engine-out hydrocarbons [12] and soot [13,14]. Soot contributes to at least 10% of ambient particulate matter [15,16], which is one of the main reasons for reduced life expectancy worldwide [17]. A further strategy is the precise adjustment of chemical properties by HP. In 2018, Haldor Topsøe announced an isomerization process to upgrade synthetic gasoline [18]. To some extent, isomerization converts durene into other isomers. In this manner, crystallization can be avoided, however, without simultaneously addressing negative emission tendencies. Sooting behavior is expressed in the literature by parameters such as the Threshold Sooting Index [19] or the Novel Yield Sooting Index [14]. Generally, naphthenes and paraffins tend to form less soot [20]. Therefore, we decided to convert the heavy aromatics into saturated compounds using HP. An additional advantage is the possibility of co-processing with fossil feedstocks, as hydrotreating and hydrocracking units are available in modern oil refineries.

The object of this paper is a process approach in which the heavy aromatics are separated, converted by HP, and finally blended back into the original gasoline. We show how a deft catalyst choice can provide high-quality gasoline free of heavy aromatics like durene. For this purpose, we

varied the reaction temperature and space velocity over a wide range and investigated how the petrochemical parameters changed. In this regard, we also briefly discuss the catalytic processes involved.

2 Greenhouse Gas Neutral Gasoline Supply in a Refinery

2.1 Processes for the Production of Synthetic Gasoline

For the production of synthetic gasoline, there are various processes. In this study, MTG and DTG are considered, which are indirect catalytic processes using methanol and dimethyl ether (DME), respectively. Both processes are based on Mobil Oil's discovery in the 1970 s that methanol can be catalytically converted to hydrocarbons by a ZSM-5 zeolite [10]. The ZSM-5 zeolite has pores of medium size at relatively high acid strength, which determines its selectivity to products in the boiling range of gasoline [21]. Almost similar product spectra are observed for the MTG and DTG processes, consisting of paraffins, olefins, and especially methylated aromatics [22]. The bioliq® DTG raw gasoline is characterized by a high concentration of aromatics (approx. 75 wt.%), leading to a low proportion of light ends with boiling temperatures up to 150°C [23]. Such fuels are suitable for gasoline engines since the high aromatic concentration is accompanied by an increased octane number [10, 22]. The aromatic distribution ranges from C_6 to C_{10} and has a maximum at C_8. Depending on the synthesis conditions, the product contains 3 wt.%–6 wt.% of durene, while the concentration in fossil gasoline is only 0.2 wt.%–0.3 wt.% [10].

DTG offers an economic advantage over MTG due to lower investment costs. It is directly based on synthesis gas and does not need methanol as an intermediate product [24]. Furthermore, the increased economic efficiency results from the sequential reactions involved. Methanol formed in the equilibrium reaction (1) reacts directly to DME in reaction (2), which accelerates the conversion of synthesis gas due to the constant removal of the intermediate product methanol [25].

$$CO + 2H_2 \rightleftharpoons CH_3OH, \quad \Delta H^0_{R,298} = -182 \text{ kJ mol}^{-1} \tag{1}$$

$$2CH_3OH \rightleftharpoons CH_3OCH_3 + H_2O, \quad \Delta H^0_{R,298} = -23 \text{ kJ mol}^{-1} \tag{2}$$

In addition, the water formed in reaction (2) is converted with carbon monoxide by the water-gas shift reaction (3). This further increases the driving force, since the hydrogen formed is involved in the methanol synthesis of reaction (1) [26].

$$H_2O + CO \rightleftharpoons H_2 + CO_2, \quad \Delta H^0_{R,298} = -41 \text{ kJ mol}^{-1} \tag{3}$$

Consequently, the conversion is higher and the resulting recycle flow is lower, further reducing operating costs [27].

The feasibility of direct DME synthesis has already been demonstrated by companies such as JFE Holdings Inc., starting operation in 1999 in Hokkaido, Japan, and Haldor Topsøe A/S in Houston, USA [28]. On a pilot scale, the bioliq® process, developed at the Karlsruhe Institute of Technology (KIT) allows the conversion of low-grade lignocellulosic biomass into synthetic fuels [29,30]. As shown in Fig. 1, raw materials such as residual waste wood or straw are collected and liquified in regional fast-pyrolysis plants [31].

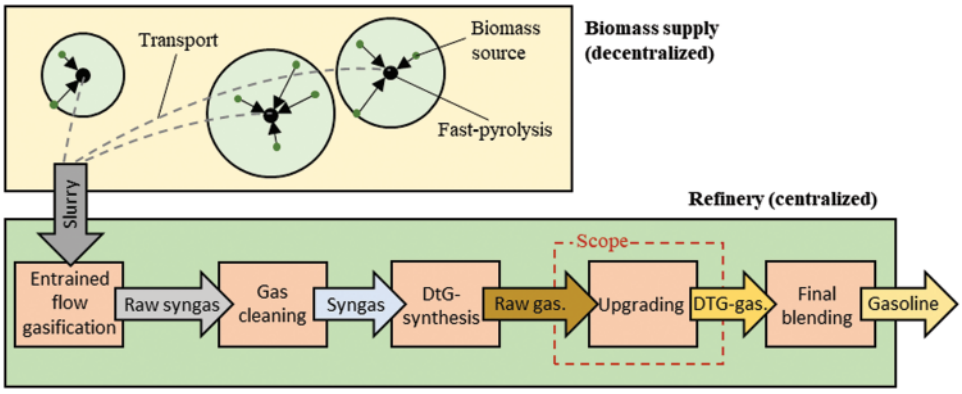

Figure 1: Production of synthetic gasoline using the bioliq® process. The biomass supply is decentralized and the DTG synthesis is centralized. Highlighted in red is the scope of this study, the upgrading of a DTG gasoline

The fast pyrolysis produces a slurry with ten times the energy density of the original biomass, resulting in lower transportation costs. In a central refinery, the slurry is converted into raw synthesis gas in an entrained flow gasifier [32]. Particulates and acid gas are subsequently removed in several gas purification stages to supply the refinery with high-quality, sulfur-free synthesis gas [30]. In the bioliq® process, the synthesis gas is fed to a DTG synthesis to produce raw gasoline [23]. Detailed considerations of efficiency and production cost estimates of the bioliq® process can be found in the work of Haro et al. [28] and Henrich et al. [33]. Regardless of their origin, synthetic DTG fuels do not necessarily meet motor gasoline standards. A further downstream upgrading is inevitably required. The upgraded DTG gasoline is piped into a blending unit, where it is mixed with additives such as ethanol or other hydrocarbon streams.

2.2 Upgrading Strategy for a Synthetic MTG/DTG Gasoline

In this study, we consider DTG gasoline from the bioliq® pilot plant at KIT in Karlsruhe, Germany. The standard DIN EN 228 must be met for gasoline in Germany [34]. Table 1 shows the petrochemical parameters of the raw gasoline as obtained directly from the bioliq® DTG synthesis. Compared with DIN EN 228, it can be seen that the boiling characteristics *E70*, *E100*, and *E150* are too low, which is equivalent to a shortage of light ends. These values indicate the volume fraction evaporated at a given temperature during distillation. For example, the measured value *E70* is the volume fraction evaporated at 70°C. The aromatic concentration significantly exceeds the permissible upper limit of 35 vol.%. Due to the high aromatic concentration, the density ρ is too high and the vapor pressure p_v is too low. It can be concluded that a stream containing an appropriate high proportion of saturated light ends is required to improve boiling characteristics while lowering the aromatic concentration.

We decided to upgrade the heavy gasoline in a downstream process by HP. As shown in Fig. 2, the total volume of raw gasoline is split into two-thirds light and one-third heavy gasoline by an atmospheric rectification.

Table 1: Petrochemical parameters of bioliq® raw gasoline, light gasoline, and heavy gasoline after rectification compared to DIN EN 228 standard [34]

Parameter	Unit	DIN EN 228	Raw gasoline bioliq®	Light gasoline bioliq®	Heavy gasoline bioliq®
RON	–	min. 95	N/A	101.7	N/A
MON	–	min. 85	N/A	93.7	N/A
ρ	kg m^{-3}	720.0–775.0	845.76	828.91	891.72
p_v (Class A)	kPa	45–60	45 ± 4	31 ± 5	0.15 ± 0.15
E70	vol.%	22.0–50.0	1.2 ± 0.7	1.1 ± 0.7	0.0
E100	vol.%	46.0–72.0	5.7 ± 0.7	6.4 ± 0.7	0.0
E150	vol.%	75.0	46.4 ± 0.7	85.4 ± 0.7	0.0
FBP	°C	210	245 ± 4	171 ± 4	290 ± 4
φ_{Benzene}	vol.%	max. 1.00	1.2 ± 0.7	1.6 ± 0.7	0.0
φ_{Olefins}	vol.%	max. 18.0	1.3 ± 0.1	1.1 ± 0.1	traces
$\varphi_{\text{Aromatics}}$	vol.%	max. 35	82.3 ± 0.7	76.3 ± 0.7	96.5 ± 0.7
$w_{\text{Oxygenates}}$	wt.%	max. 3.7	traces	traces	0.0

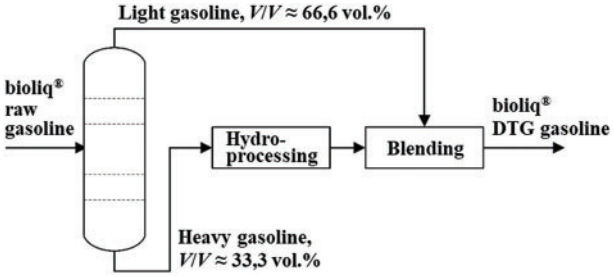

Figure 2: Schematic flow diagram for upgrading an MTG/DTG gasoline. The upgrading process consists of a rectification column, a hydroprocessing reactor, and a blending unit that yields the final DTG product by blending the light and the upgraded heavy gasoline

The petrochemical parameters for both fractions obtained by rectification are listed in Table 1. Due to its high concentration of aromatics (1.7 vol.% benzene, 17.2 vol.% toluene, 43.2 vol.% xylenes, 15.1 vol.% trimethylbenzens), bioliq® light gasoline is considered a valuable blending component. As shown in Fig. 2, we forward the heavy gasoline to a HP unit where the petrochemical parameters are adjusted accordingly. This fraction is then piped into a blending unit, where it is blended back into the light gasoline. In addition to adjusting the above parameters, the Research Octane Number (*RON*) and Motor Octane Number (*MON*) of the hydroprocessed heavy gasoline should remain as high as possible. Otherwise, there is a risk that the octane numbers of the blend will fall below the specifications required by DIN EN 228. Maintaining octane numbers can be challenging because saturated hydrocarbons usually have lower ones than aromatics [13]. If there is no volume loss during HP, the ratio of light to upgraded heavy gasoline must remain 2:1 as delivered during rectification. Table 1 shows that nearly 97 vol.% (96.95 wt.%) of the heavy gasoline is composed of aromatic hydrocarbons. At approx. 52.6 wt.%, the largest proportion consists of C_{10} (21.4 wt.% durene) and

approx. 10.4 wt.% of C_{12} aromatics. Accounting for 33.6 wt.%, the C_9 aromatics have the second largest share. The remaining 3 wt.% are mostly naphthenic. Measured data on the exact feed composition can be found in Table A1 in the Appendix A.

2.3 Hydroprocessing of Streams Rich in Heavy Aromatics

HP is a promising process for converting heavy aromatic hydrocarbons into light and saturated molecules. The term HP is used for different reactions with hydrogen. Depending on the process conditions and the chosen catalysts, this includes hydrogenation, hydrocracking, and hydroisomerization. Which reaction regime is most promising for a given feedstock depends on how the target petrochemical parameters are to be adjusted.

Depending on the used catalyst, hydrocracking can follow four reaction pathways, i.e., hydrocracking over bifunctional catalysts, hydrogenolysis on metal sites, catalytic hydrocracking on monofunctional catalysts (also referred to as Haag-Dessau mechanism), and thermal hydrocracking [35]. By using a bifunctional metal/zeolite catalyst, hydrocracking allows almost complete hydrogenation of aromatics in one reaction step. Simultaneously, a certain amount of highly branched naphthenes and paraffins are formed [36]. The saturated products have lower boiling temperatures than aromatics with the same number of carbon atoms. A further lowering of the boiling temperatures results from the formation of low-molecular cracking products.

Noble metals are particularly suitable as active sites for deep aromatic saturation. They can achieve high hydrogenation activities even at relatively low temperatures, where the thermodynamic equilibrium is on the side of the saturated products [37]. Therefore, the hydrogen pressure can be kept low. This maintains some flexibility in terms of operating temperature and pressure [38]. The latter is important because biomass-derived fuels are variable and contain a wide range of hydrocarbons that are not easily hydrogenated. With the operating temperature, the yield of light ends can be adjusted. The catalyst support must be chosen accordingly. Figueras et al. [39] described how the presence of an acidic support induced an electron deficit in palladium and thereby accelerated the benzene hydrogenation. Moreover, Tri et al. [40] explained the influence on the selectivity of co-hydrogenation of a benzene-toluene mixture by the electrophilic character of platinum resulting from the support's acidity. Due to their sufficient acidity, aluminosilicates are beneficial as catalytic supports. More precisely, the subgroup zeolites are in particular suitable for HP. An advantage over their forerunners in acid-catalyzed reactions, i.e., amorphous silica-alumina, is the superior acid strength of zeolites [41]. Further beneficial is the possible formation of selectively desired products by steric constraints within their structural environment [42]. Naphthenes, resulting from the hydrogenation of aromatics, can undergo sequential reactions. Mignard et al. [43] studied the reaction of methylcyclohexane (MCH) over a bifunctional Pt/USY catalyst. They observed that naphthenes undergo a ring contraction (RC) reaction, where C_6 rings shrink to C_5 rings while the molar mass remains constant. Figueras et al. [44], studying the RC reaction of MCH over platinum impregnated sulfated zirconias, showed that the distribution of acid strength has the greatest influence on selectivity and activity. Weitkamp et al. [45] also used MCH as probe molecule over Pt/HZSM-5, Pt/CaY, and Pd/LaY, among other naphthenes. Based on the isomer distribution, they demonstrated the shape selective influence of the zeolite structure, as some isomers were not found in the product mixture for HZSM-5. Using a Pt-Ir/ZrO_2-SO_4^{2-} and a pure ZrO_2-SO_4^{2-} catalyst, Belatel et al. [46] suggested that besides an acid site, a metal component also plays an active role in the isomerization process of MCH. The dehydrogenation at the metal site leads to a cycloalkene, which is protonated at a Brønsted acid site, yielding a (cyclic) carbenium ion [35]. RC leads to a variety of isomers that increase with the number of carbon atoms in the naphthene. The isomers differ considerably in their petrochemical parameters such as octane number [47], but the boiling temperatures also vary within a certain range.

For a better understanding, Fig. 3 shows the typical reaction pathways for the HP of aromatic hydrocarbons using the example of durene, since it is the substance with the highest concentration in the feed.

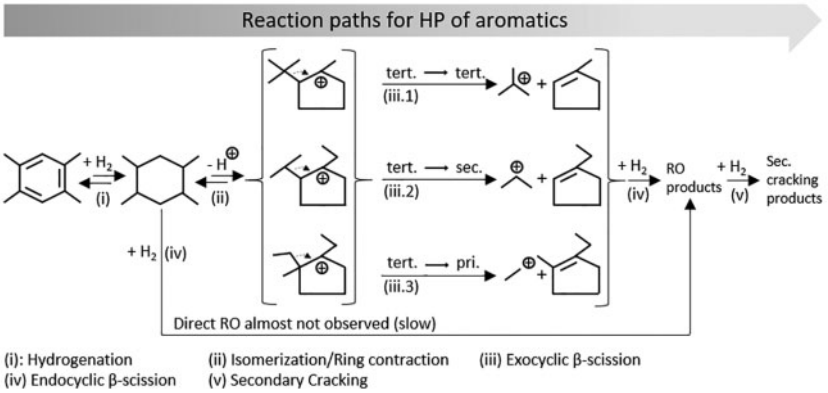

Figure 3: Reaction pathways for HP of durene, including (i) Hydrogenation, (ii) Isomerization/Ring contraction, (iii) Exocyclic β-scission, (iv) Endocyclic β-scission, and (v) Secondary cracking

Reaction (i) shows the hydrogenation of durene, followed by RC in reaction (ii). It should be noted that many other isomers can be formed, e.g., two methyl groups instead of one ethyl group attached to the ring at different positions. As explained above, the distribution is highly dependent on a) the acid strength distribution and b) the shape selective influence of the used catalyst. Besides hydrogenation and RC, β-scission of endo-and exocyclic carbon-carbon bonds are important reactions in bifunctional hydrocracking. Both reactions proceed via the formation of a carbenium ion. However, it can be stated that endocyclic carbon-carbon bonds are more difficult to break and the reaction is correspondingly slower [48]. Brouwer et al. [49] found the cause in the unfavorable orientation of the p-orbital of a positively charged carbon atom to the C-C bond to be broken. Endocyclic β-scission, also called ring opening (RO), yields paraffins. In general, RC products can subsequently be ring opened. Reaction (ii) shows the rearrangement of carbon atoms, which allows the formation of a stable tertiary cyclic carbenium ion in the ring structure. For naphthenes $\geq C_{10}$, the fast tertiary-tertiary β-scission is the predominant reaction, yielding an iso-butyl carbenium ion and methylcyclopentene (in case of durene) as products (reaction iii.1). Egan et al. [50] referred to this reaction as the paring reaction. Interestingly, the product spectrum of the paring reaction proved to be independent of the isomer configuration of the reactant [51]. It can be concluded that isomerization reactions (endo- and exocyclic alkyl shifts) are faster than exocyclic β-scission. Reactions (iii.2) and (iii.3) describe the tertiary-secondary and the tertiary-primary exocyclic β-scission of a C_{10} naphthene. The resulting secondary and primary carbenium ions lead to the formation of the products propane and ethane after a final hydrogen transfer. In an uninhibited reaction, the rates decrease in the order: tertiary-tertiary > tertiary-secondary > tertiary-primary, according to the stability of the respective carbenium ions. However, this might be influenced by shape selective constraints of the zeolites used on the bulky intermediates. As a result, a slower mechanism incorporating less spacious intermediates may be favored over the fast paring mechanism. Naphthenes $< C_9$ can only follow reaction pathways via the formation of secondary and primary carbenium ions, since tertiary-tertiary exocyclic β-scission is mechanistically hindered.

Bifunctional hydrocracking gained increased interest with the growing demand for fuels. Polynuclear aromatics are the least desirable products in diesel fuels. Besides too high densities, unfavorable cold-flow properties, and low cetane numbers [52], they also exhibit too high emission tendencies. Several approaches exist, one of which is the selective RO to yield products with high cetane numbers while maintaining high fuel yields [52–54]. The same considerations were made for heavy mononuclear aromatics in gasoline. Lower densities, higher octane numbers, and better combustion characteristics are possible when the rings are opened to form branched paraffins [47,55–57].

3 Material and Methods

In this study, a lab scale HP setup with a maximum throughput of approx. 7.2 L d^{-1} was used. As shown in Fig. 4, a fixed bed reactor with an inner diameter of 14.9 mm, was operated top-down in co-current mode. The reactor was electrically heated using three heat brackets.

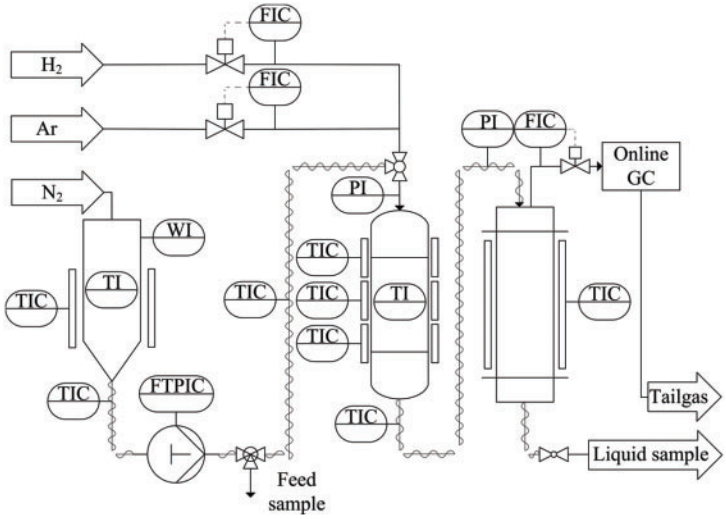

Figure 4: Flow diagram of the laboratory HP setup used in this study

A central probe tube with an outer diameter of 1/8″ was available to measure the catalyst bed temperature by axially moving a K-type thermocouple. Clariant AG loaded the three pelletized commercial catalysts with 0.3 wt.% platinum. The hand-grinded and sieved 100–200 µm fraction was diluted with silicon carbide of the same particle size distribution in a ratio of approx. 1:2 (V/V) and filled into the reactor between two further layers of pure silicon carbide. Table 2 lists the catalysts used in this work.

Table 2: Catalysts used for the experiments

Metal and Zeolite	Metal loading in wt.%	Catalyst mass in g	Bed height in mm
Pt/HZSM-5	0.3	12.694	405
Pt/Mordenite	0.3	12.689	466
Pt/SAPO-11	0.3	20.005	453

Catalyst bulk densities, and thus bed heights, varied due to the manual grinding process. Since the activity of Pt/SAPO-11 was the lowest observed, the catalyst mass was increased. This resulted from the need to produce large sample quantities for the analysis of the petrochemical parameters. The feed was placed in a storage tank tempered to 50°C to keep the durene dissolved. To build up the reaction pressure on the liquid side and to pipe the heavy gasoline at a flow rate of 0.01–5.00 mL min^{-1}, a Bischoff HPD pump–Multitherm 3351 heated to 50°C was used. In addition to the liquid feed, the gas was also fed to the top of the reactor. The H_2 with a purity of 99.999% was metered with a Bronkhorst EL-Flow® Select mass flow controller (MFC) and premixed with the liquid phase in the first 20 cm of the fixed bed, which consisted of pure silicon carbide and was tempered to reaction temperature. In a downstream separator with a volume of approx. 800 mL, the liquid-gas product mixture was separated at ambient temperature and reaction pressure. The liquid product was drawn off at the bottom of the separator via a cooling coil tempered to 0°C, in order that no noticeable pressure drop occurred in the reactor. The extracted liquid product was stored gas-tight at below 0°C and analyzed offline according to the parameters specified in DIN EN 228. A Reformulyzer M4 from the company PAC and an Agilent gas chromatograph (GC) 7890A calibrated according to ASTM D6730–01 [58] were used to measure the compositions of the liquid hydrocarbon samples. The Reformulyzer M4 provided a comprehensive insight into the sample by having the instrument distinguish between groups of substances and the number of carbon atoms. To measure individual components, e.g., the concentration of durene, the Agilent 7890A GC was used as a complementary method. *RON* and *MON* were determined following ISO 5164 [59] and ISO 5163 [60], respectively, by PetroLab in Speyer, Germany, using a frequently inspected Cooperative Fuel Research (CFR) test engine. In addition, octane numbers were measured using a PAC OptiFuel based on an infrared measurement followed by automatic spectrum analysis. Since the hydrocarbon mixtures studied were either rich in aromatics (feed) or naphthenes (products), the model underlying the OptiFuel was extended as part of the work. Octane numbers measured with a CFR test engine were used to train the new model, and a certain number of samples were retained for validation. An error of ±4 and ±2 could be determined for the *RON* and the *MON*, respectively. The calculation of the *E70*, *E100*, and *E150* values according to DIN EN 228 was based on the boiling curve measured with a PAC OptiDist calibrated according to ASTM D86 [61] for sample volumes > 100 mL or a PAC OptiPMD calibrated according to ASTM D7345 [62] for sample volumes < 100 mL. By interpolation between two measuring points recorded with a resolution of 1 vol.%, *E70*, *E100*, and *E150* were calculated. The vapor pressure was measured using a PAC Herzog HVP 972 according to ASTM D6378 [63] at 37.8°C. Finally, the density was measured at 15°C according to a self-developed method utilizing a Mettler&Toledo D5. The gas stream leaving the separator was directed to a Bronkhorst EL-Press® MFC, which was used to control the reaction pressure. Subsequently, it was depressurized to atmospheric pressure and fed into an Agilent 7890A GC. To calculate the mass balance, argon with a purity of 99.999% was fed as internal standard into the top of the reactor, using a Bronkhorst EL-Flow® Select MFC. Based on the change in argon concentration due to the reactions between the feedstock and hydrogen, the total outlet volume flow could be calculated.

Additional experiments were conducted in a self-designed batch reactor. The reactor was equipped with a hydrogen inlet by which the reaction pressure was adjusted. A heating jacket provided the necessary heat, while there was no cooling option. The hydrogen was dispersed into the liquid phase with a self-priming stirrer operated at 800 min^{-1}. Liquid samples were taken after specific time intervals and analyzed offline using the Agilent 7890A GC as described above. A model mixture of 27.1 wt.% toluene, 31.2 wt.% xylene isomers, 35.3 wt.% 1, 2, 4-trimethylbenzene and 6.3 wt.% 1,

2, 4, 5-tetramethlybenzene was used as feed. For each experiment, 0.3 g catalyst with a particle size distribution of 20–63 µm was added to 70 g of feed.

All measurements were repeated whenever possible and statistically evaluated according to the student's t-distribution, assuming a 95% confidence interval.

4 Results

4.1 Adjustment of Petrochemical Parameters

As shown in Fig. 5, several gasoline qualities were produced by HP bioliq® heavy gasoline with a fixed bed reactor to investigate how the petrochemical parameters can be adjusted. Fig. 5a shows the heavy gasoline stored at approx. 20°C (left) and 0°C (right). A representative product fraction after HP can be seen in Fig. 5b. Comparing Figs. 5a and 5b qualitatively shows the effect of HP the heavy gasoline. While the durene forms crystals in the heavy gasoline at 0°C there is nothing such observed after HP.

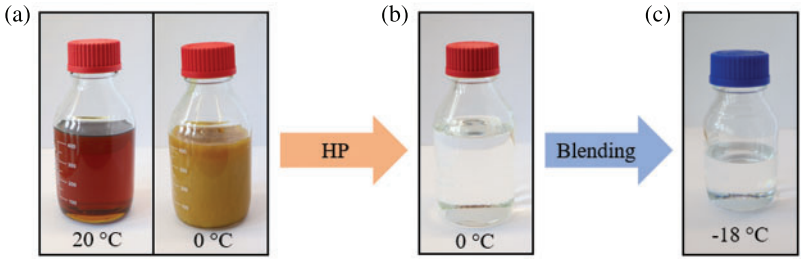

Figure 5: (a) bioliq® heavy gasoline, (b) product after HP with Pt/HZSM-5 ($p = 50$ bar, $T = 270$°C and $WHSV = 1.39\ h^{-1}$) and (c) bioliq® blend as discussed in the blending section, stored at temperatures as indicated in the respective image

For each experiment, a target temperature T_{target} for the catalyst bed was set. Due to the exothermic nature of the hydrogenation reaction, it was not possible to provide fully isothermal conditions. $T_{FB,min}$ and $T_{FB,max}$ are the minimum and maximum temperatures measured in the fixed bed and provided in the Appendix, if measured. As explained in the theoretical part on HP, cracking reactions lead to the formation of gaseous products, which reduces the yield of products in the boiling range of gasoline. The decision for a particular operating point is therefore not based solely on the maximum achievable quality of the product, but requires a comparison to the gasoline yield as defined by Eq. (4).

$$Y_{Gasoline} = \frac{\dot{m}_{Gasoline}}{\dot{m}_{Feed}} \tag{4}$$

Therefore, the petrochemical parameters to be optimized are discussed as a function of the gasoline yield. The pressures for the experiments were set to achieve an almost complete conversion of the aromatics. Table 3 shows the parameter ranges investigated for each catalyst. The Pt/HZSM-5 catalyst exhibited the highest hydrogenation activity, based on the applied pressures. An almost complete conversion of aromatics was achieved at a pressure of 50 bar.

Table 3: Parameter ranges investigated with the catalysts

	Pt/HZSM-5	Pt/Mordenite	Pt/SAPO-11
T in °C	230–330	250–270	270–350
p in bar	50–70	90	90
$WHSV$ in h^{-1}	0.84–2.66	1.39	1.39 and 0.88

For the other catalysts Pt/SAPO-11 and Pt/Mordenite, a pressure of up to 90 bar was required. Due to equilibrium limitations at temperatures of ≥310°C, the *WHSV* had to be additionally reduced from 1.39 h^{-1} to 0.88 h^{-1} for Pt/SAPO-11. Data obtained from the CFR motor experiments and FTIR measurements are used for evaluating the *MON* and *RON*. The standard deviation of ±4 for *RON*-FTIR measurements is considered too high. Therefore, these data are not used in this study, and no *RON* values can be reported for experiments with Pt/SAPO-11 since no CFR measurements were performed. The octane numbers measured in this study, as a function of various parameters, are displayed in Fig. 6. Fig. 6a shows the MON and RON as a function of the gasoline yield.

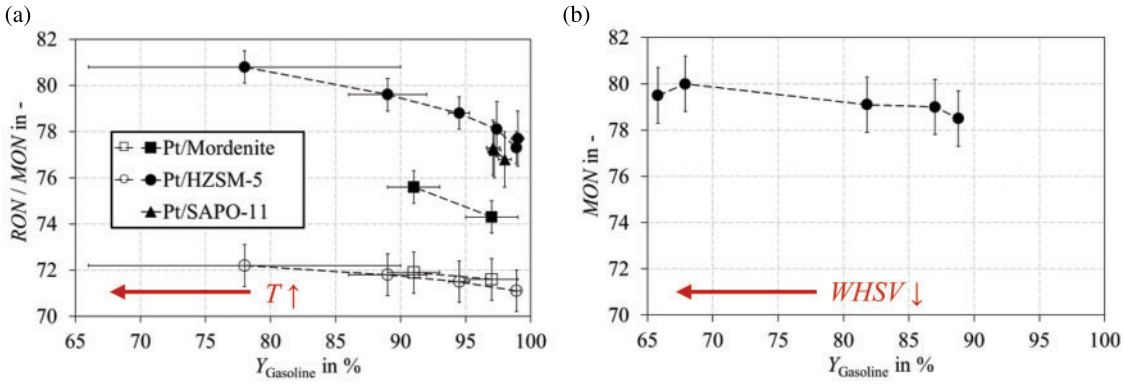

Figure 6: *RON* (white symbols) and *MON* (black symbols) as a function of gasoline yield, adjusted (a) by reaction temperature and (b) by space velocity. Experiments with Pt/Mordenite, Pt/HZSM-5, and Pt/SAPO-11 were performed in a fixed bed reactor according to the parameters listed in Table B1 (*T* variation) and Table B2 (*WHSV* variation) in Appendix B

Pressure and space velocity were kept constant during the experiments, while the gasoline yield was adjusted by varying the reaction temperature. The corresponding data can be found in Appendix B. Throughout the investigated parameter range, *MON* consistently exceeds *RON*, which is probably due to the samples' high C_9 and C_{10} naphthene content. For Pt/HZSM-5, the *MON* increases by 3.5 between a gasoline yield of 99 wt.% and 78 wt.%, while only by 1.1 for the *RON*. Compared to a *MON* of 85, as required by DIN EN 228, the measured values of up to 80 are promising. On the other hand, measured *RON* values of up to 72 do not meet 95 as demanded by the standard. However, it can be stated that the overall *RON* and *MON* values are favorable, as naphthenes larger C_9 are typically < 35 and < 30, respectively [64]. The *MON* varies depending on the catalyst used. It can be observed that the *MON* increases in the order: Pt/HZSM-5 > Pt/SAPO-11 > Pt/Mordenite. The selective isomerization of naphthenes explains these results since, especially at high gasoline yields of 97 wt.%–100 wt.%, hardly any paraffins are formed besides a negligible concentration of aromatics. McVicker et al. [65] found the same order as reported above for the RC of MCH expressed as the

1, 2-dimethylcyclopentane (DMCP)/1, 3-DMCP ratio. For Pt/HZSM-5, almost no 1, 2-DMCP was formed, whereas the isomer distribution was almost in equilibrium for Pt/Mordenite. In conclusion, the differences in *MON* values can clearly be attributed to the shape selective influence of the catalysts.

In contrast to the *MON*, no dependency on the catalyst selectivity is evident for the *RON* in the studied parameter range. The values obtained by the CFR engine are nearly congruent for Pt/Mordenite and Pt/HZSM-5. This is probably due to the less harsh test conditions for *RON* measurements, since the degree of isomerization and thus the thermal stability of the molecule does not play such a crucial role. In addition, the produced samples do not correspond to any standard fuel. The sample matrix and thus the high content of naphthenes must be considered. Considering the *MON* values for Pt/SAPO-11 lying between those of the other two investigated catalysts, it can be assumed that the *RON* values for Pt/SAPO-11 are comparable to those of Pt/Mordenite and Pt/HZSM-5.

Fig. 6b shows the *MON* for a constant reaction temperature of 330°C at a pressure of 60 bar for Pt/HZSM-5 under variation of the *WHSV*. In contrast to Fig. 6a, the *MON* does not increase as distinct. Fig. 7 shows the gasoline composition for both experiments carried out with Pt/HZSM-5 under variation of temperature (black symbols) and space velocity (white symbols).

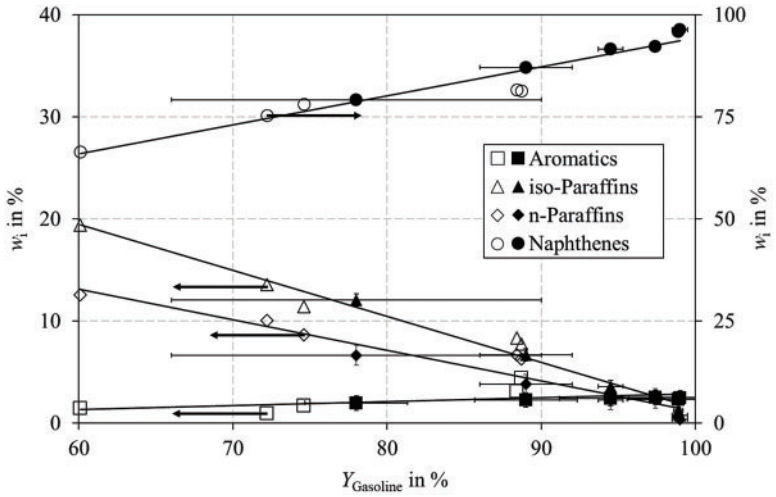

Figure 7: Gasoline composition plotted against gasoline yield for the experiments conducted under variation of the reaction temperature (black symbols) and *WHSV* (white symbols) for Pt/HZSM-5. Experiments with Pt/HZSM-5 were performed in a fixed bed reactor according to the parameters listed in Table B1 (*T* variation) and Table B2 (*WHSV* variation) in Appendix B

The fractions can be described with sufficient agreement by straight lines. In the experiments under variation of the *WHSV* (white symbols), the increasing yield of iso-paraffins does not drive the octane numbers as expected (Fig. 6b). We believe that the RC of naphthenes due to elevated reaction temperatures is responsible for the observed increase in the octane numbers, rather than the iso-paraffin yield. As described in materials and methods, we performed additional HP experiments in a batch reactor with a model mixture of aromatics and calculated the RC for the C_7 naphthenes according to Eq. (5) to prove this statement.

$$x_{RC,C7} = \frac{\sum x_{DMCP-isomers} + x_{ECP}}{\sum x_{C_7-Naphthenes}} \quad (5)$$

The RC of MCH is a well-known model reaction in the literature due to the accessible product spectrum [13,43,45,47,65]. During RC of MCH (hydrogenation product of toluene), DMCP isomers and ethylcyclopentane (ECP) are formed. Fig. 8 shows the RC as a function of time (Fig. 8a) and reaction temperature (Fig. 8b) for Pt/HZSM-5 and Pt/Mordenite. No RC was observed for Pt/SAPO-11 in the investigated temperature range.

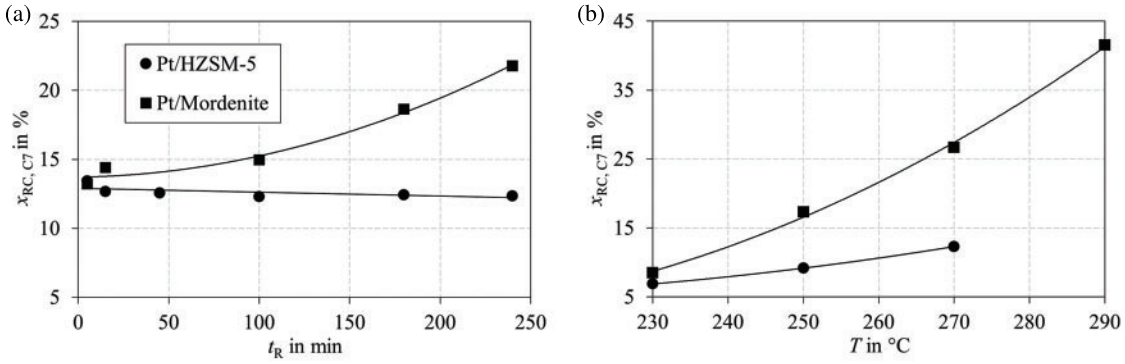

Figure 8: RC of MCH at a pressure of 50 bar for Pt/HZSM-5 and Pt/Mordenite measured in a batch reactor (a) as a function of reaction time at a temperature of 270°C and (b) as a function of temperature for a reaction time of 100 min

It is remarkable how fast the RC products in Fig. 8a for Pt/HZSM-5 reach a steady state, while the RC reaction for Pt/Mordenite still proceeds after four hours. This can be linked to the observations in Fig. 6b, where no clear dependence of *MON* on *WHSV* is seen for Pt/HZSM-5. In Fig. 8b, the temperature influence is shown on the RC. The RC products increase over the reaction temperature for both catalysts, which is especially pronounced for Pt/Mordenite. A dependence on reaction temperature was also described by Belatel et al. [46]. The degree of secondary isomerization of ECP to DMCP was strongly connected to the reaction temperature in their experiments. Overall, we conclude that the RC of naphthenes originating from the primary hydrogenation of aromatics and from exocyclic β-scission is responsible for increased octane numbers.

One main objective of this study is the production of light ends from heavy gasoline. The description of the HP reactions in Fig. 3 is recommended to better understand the following discussions of the cracking mechanisms. Fig. 9 illustrates the boiling characteristics *E70*, *E100*, and *E150* as defined according to DIN EN 228 and the additional value *E180*. The *E150* and *E100* benefit most clearly from cracking. At a gasoline yield of 90% using Pt/HZSM-5, the *E150* increases to almost 40 vol.%. A similarly sharp rise is observed for Pt/Mordenite. However, only two points were measured here. Pt/SAPO-11, on the other hand, shows only a slight cracking activity in the investigated temperature range. Most probably, the sharp increases in *E150* and *E100* are due to fast tertiary-tertiary exocyclic β-scission (paring reaction) of C_{10} naphthenes resulting in the production of C_6 naphthenes and iso-butane. The slightly higher *E100* for Pt/HZSM-5 than for Pt/Mordenite for all measured data points can be attributed to the shape selective influence of the zeolites. The narrower pores of HZSM-5 sterically hindered the paring reaction. This was verified by a high yield of C_5 paraffins in the product spectrum, which were almost not observed with Pt/Mordenite. C_5 paraffins are formed by the slow direct ring opening of C_9 and C_{10} naphthenes, followed by secondary cracking of the resulting paraffins. Direct RO results in a higher gasoline yield because less C_4 is formed. The same applies to the *E70*, which also benefits from an increased C_5 yield. The *E150* also benefits from the slower

tertiary-secondary and tertiary-primary exocyclic β-scission. This was verified by a high yield of C_6-C_8 naphthenes and corresponding ethane and propane in the product stream. The difference between the bioliq® raw gasoline and DIN EN 228 is particularly pronounced in the case of *E70* and is therefore the most crucial parameter. The proportion of light ends with a boiling temperature of up to 70°C is 1.2 vol.%, while the standard requires at least 22 vol.% (see Table 1). This parameter increases slowly for a decreasing gasoline yield and rises sharply at approx. 88 wt.%. The observed is probably due to the slow endocyclic β-scission (ring opening) of C_6 naphthenes previously formed by exocyclic β-scission, producing hexanes. From a process engineering point of view, the range below a mass yield of 90% is excluded because of the high carbon loss due to cracking.

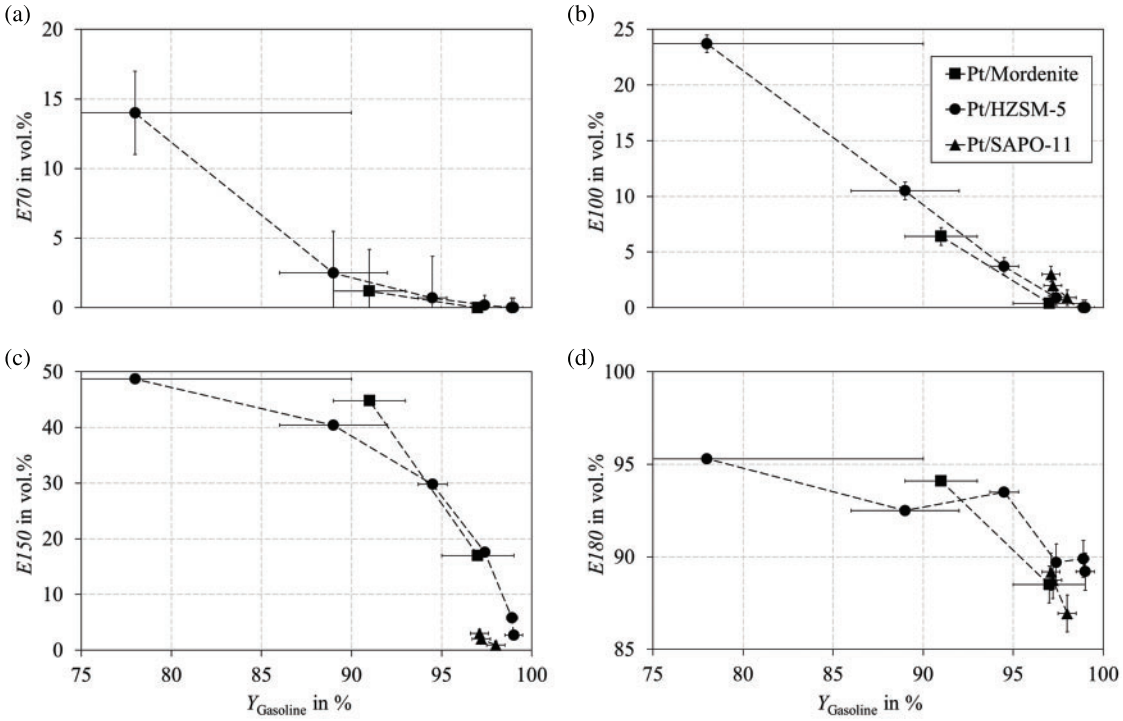

Figure 9: Boiling characteristics (a) *E70*, (b) *E100*, (c) *E150*, and (d) *E180* plotted against the gasoline yield. Experiments performed with Pt/Mordenite, Pt/HZSM-5, and Pt/SAPO-11 in a fixed bed reactor according to the parameters listed in Table B1 in Appendix B under variation of the reaction temperature

Table 1 shows further optimization potential for the density and vapor pressure of the bioliq® raw gasoline, which are too high and too low, respectively. Fig. 10 shows how the density and vapor pressure change with the gasoline yield. An almost linear relationship with gasoline yield can be observed for both parameters. The density decreases and the vapor pressure increases as a result of cracking reactions. Low molecular ring structures and paraffins lead to the observed trends in Fig. 10, which can also be seen in Fig. 7. There is little influence of the catalysts used on both parameters. The observed trends for the boiling characteristics in Fig. 9 can be applied to density and vapor pressure. For Pt/SAPO-11, a slightly higher density and lower vapor pressure result from lower cracking activity.

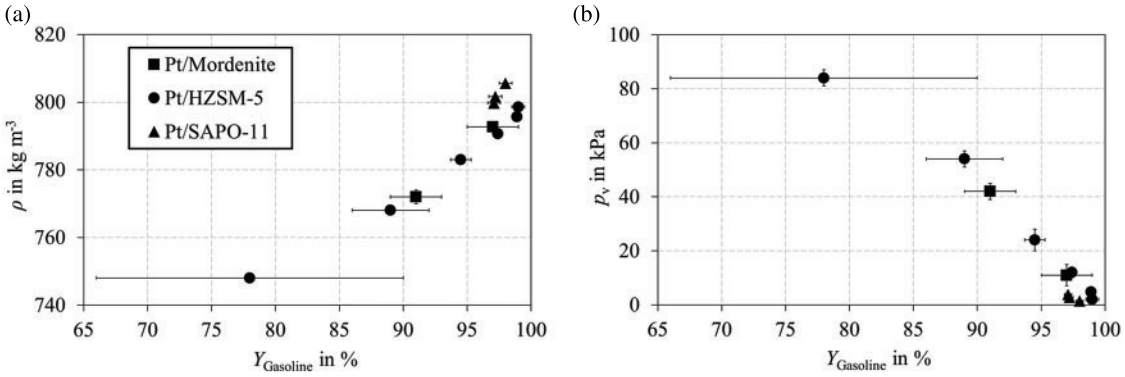

Figure 10: (a) Density and (b) vapor pressure plotted against the gasoline yield. Experiments with Pt/Mordenite, Pt/HZSM-5, and Pt/SAPO-11 were performed in a fixed bed reactor according to the parameters listed in Table B1 in Appendix B under variation of the reaction temperature

4.2 Blending

For a final discussion, we conducted blending experiments with the bioliq® light gasoline and the upgraded heavy gasoline. The heavy gasoline was upgraded in a fixed bed reactor with a capacity of 1 L h^{-1} filled with 0.3 wt.% Pt/HZSM-5 pellets. The product was comparable to the quality obtained in the lab scale experiments discussed above, except that it was rectified to a *FBP* of approx. 170°C. The bioliq® blend consisted of two-thirds light gasoline and one-third upgraded heavy gasoline, as this was the original volume ratio of light to heavy gasoline after separation following the bioliq® DTG synthesis. All relevant data, such as composition, can be found in Appendix C. An image of the final blend at −18°C is shown in Fig. 5c. No crystals formed as a result of durene removal, indicating the gasoline's operability under cold conditions. Fig. 11 shows the bioliq® raw gasoline in comparison with the blend. The most obvious change can be seen for the *FBP*, which results from the applied rectification. The aromatic concentration was relatively reduced by 37.5%, but remained too high compared to DIN EN 228. With the removal of most heavy aromatics and the lower *FBP* in general, a significant decrease in engine-out emissions is expected. The octane numbers of the blend decreased because the ones of the upgraded heavy gasoline were lower than those of the bioliq® light gasoline. However, both remained within the minimum values of the standard. A slight improvement can be seen in the density, which has dropped but still does not reach the limit values of DIN EN 228. The boiling characteristics *E70*, *E100*, and *E150* could be improved. In particular, the *E150* has increased significantly and meets the minimum value specified in the standard. The values for *E70* and *E100* improved slightly. If the density and vapor pressure are also considered, it becomes clear that further low-boiling components are required to meet the standard.

Up to 3.7 wt.% of O_2-equivalent oxygenates are allowed depending on the substance. Ethanol is the most popular species and is limited to 10 vol.%. In contrast, methyl tert-butyl ether and ethyl tert-butyl ether can be blended with gasoline at almost 22 vol.%, with boiling temperatures of 55.2°C and 73°C, respectively. With these considerations, *E70* could reach 22 vol.%, as specified by DIN EN 228. For adjusting the *E100*, an additional blending stream is necessary, since it is almost 36 vol.% below the minimum value of 46 vol.% defined in DIN EN 228. Methanol-to-olefin products or light ends from hydrocracked FT waxes are potentially renewable and available in a future refinery. The latter offers the possibility of co-HP with bioliq® heavy gasoline.

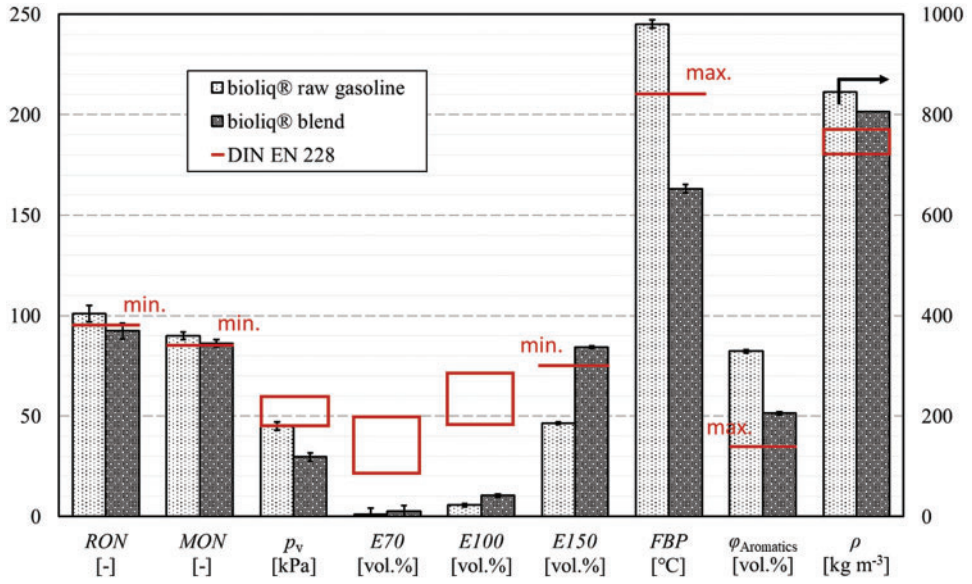

Figure 11: Petrochemical parameters of bioliq® raw gasoline and bioliq® blend in comparison with DIN EN 228

5 Conclusion

In this study, we investigated the single-stage upgrading of aromatic-rich heavy gasoline from the bioliq® process. The heavy gasoline was separated from the light gasoline and hydroprocessed using three different Pt/zeolites. Among the investigated catalysts, Pt/HZSM-5 performed the best for the purpose presented. The achieved octane numbers were the highest, which we concluded was most likely due to selective ring contraction at elevated temperatures. There was almost no difference in the yield of light ends between Pt/HZSM-5 and Pt/Mordenite. Pt/SAPO-11 showed only little cracking activity. In addition to the complete hydrogenation of the aromatic hydrocarbons, light ends with boiling temperatures up to 150°C (*E150*) and 100°C (*E100*) could be increased by approx. 40 vol.% and 10 vol.%, respectively, with a gasoline yield of 90 wt.%. Light ends were produced by fast tertiary-tertiary exocyclic β-scission, forming C_6 naphthenes and iso-butane. Moreover, the slower tertiary-secondary and tertiary-primary exocyclic β-scission, in which C_6–C_8 naphthenes and corresponding ethane and propane are formed, led to a sharp increase in *E150*. Further ring opening resulted in a slight increase in light ends with boiling temperatures up to 70°C (*E70*).

The petrochemical parameters of the bioliq® DTG gasoline were significantly improved by blending the upgraded heavy gasoline with the light gasoline. The *E150* and *FBP* of the bioliq® blend met the DIN EN 228 standard. The aromatic content was 37.5% lower than in bioliq® raw gasoline, which significantly improved the suitability as a drop-in in fossil fuels.

Acknowledgement: This publication is dedicated to the memory of Prof. Dr. rer. nat. Hans Schulz. We thank Dr. Thomas Otto and Doreen Neumann-Walter from the Institute of Catalysis Research and Technology (IKFT) as part of the Karlsruhe Institute of Technology for their strong support in characterizing the fuels. We would especially like to thank Clariant AG for providing the catalysts.

Availability of Data and Materials: All measurement data on which the diagrams presented in this study are based can be found in the Appendix.

Funding Statement: The authors acknowledge the financial support of the Federated State of Baden-Wuerttemberg for the Project reFuels–Rethinking Fuels.

Conflicts of Interest: The authors declare that they have no conflicts of interest to report regarding the present study.

References

1. European Commission (2019). Communication from the Commission of the European Parliament, the European Council, the Council, the European Economic and Social Committee and the Committee of the Regions: The European Green Deal. Brussels.
2. European Commission. Directorate General for Environment (2021). *EU biodiversity strategy for 2030: Bringing nature back into our lives.* Luxembourg: Publications Office of the European Union.
3. Petrowitsch, G., Pribil, A. (2021). Fridays for future demands climate neutral mobility and a complete mobility revolution. In: Liebl, J., Beidl, C., Maus, W. (Eds.), *Internationaler motorenkongress 2021, Proceedings*, pp. 589–595. Wiesbaden: Springer Vieweg.
4. Federal Motor Transport Authority Germany (2021). Annual report: New registrations 2021. https://www.kba.de/DE/Statistik/Fahrzeuge/Neuzulassungen/Jahresbilanz_Neuzulassungen/jahresbilanz_node.html;jsessionid=30A74ED01E115801E2E75BDF2ECAD7B2.live11292.
5. Federal Motor Transport Authority Germany (2022). Annual report: Inventory 2022. https://www.kba.de/DE/Statistik/Fahrzeuge/Bestand/Jahrebilanz_Bestand/fz_b_jahresbilanz_node.html.
6. Speight, J. G. (2020). *The refinery of the future.* Oxford: Gulf Professional Publishing.
7. Olsbye, U., Svelle, S., Bjørgen, M., Beato, P., Janssens, T. V. W. et al. (2012). Conversion of methanol to hydrocarbons: How zeolite cavity and pore size controls product selectivity. *Angewandte Chemie International Edition, 51(24),* 5810–5831. DOI 10.1002/anie.201103657.
8. Tsai, T. C., Liu, S. B., Wang, I. (1999). Disproportionation and transalkylation of alkylbenzenes over zeolite catalysts. *Applied Catalysis A: General, 181(2),* 355–398. DOI 10.1016/S0926-860X(98)00396-2.
9. Yegorov, A. S., Ivanov, V. S., Wozniak, A. I. (2014). International and Russian methods of synthesis and use of pyromellitic acid dianhydride and tendencies of their development (Review). *Biosciences Biotechnology Research Asia, 11(3),* 1765–1779. DOI 10.13005/bbra/1583.
10. Liederman, D., Yurchak, S., Kuo, J. C. W., Lee, W. (1982). Mobil methanol-to-gasoline process. *Journal of Energy, 6(5),* 340–341. DOI 10.2514/3.62614.
11. Chang, C. D. (1983). Hydrocarbons from methanol. *Catalysis Reviews Science and Engineering, 25(1),* 1–118. DOI 10.1080/01614948308078874.
12. Petit, A., Montagne, X. (1993). Effects of the gasoline composition on exhaust emissions of regulated and speciated pollutants. *SAE Technical Papers,* 932681. DOI 10.4271/932681.
13. Do, P. T. M., Crossley, S., Santikunaporn, M., Resasco, D. E. (2007). Catalytic strategies for improving specific fuel properties. *Catalysis, 20,* 33–64. DOI 10.1039/0140-0568.
14. McEnally, C. S., Pfefferle, L. D. (2007). Improved sooting tendency measurements for aromatic hydrocarbons and their implications for naphthalene formation pathways. *Combustion and Flame, 148(4),* 210–222. DOI 10.1016/j.combustflame.2006.11.003.
15. Fraser, M. P., Yue, Z. W., Tropp, R. J., Kohl, S. D., Chow, J. C. (2002). Molecular composition of organic fine particulate matter in Houston, TX. *Atmospheric Environment, 36(38),* 5751–5758. DOI 10.1016/S1352-2310(02)00725-2.

16. Zheng, M., Salmon, L. G., Schauer, J. J., Zeng, L., Kiang, C. S. et al. (2005). Seasonal trends in PM2.5 source contributions in Beijing, China. *Atmospheric Environment, 39(22),* 3967–3976. DOI 10.1016/j.atmosenv.2005.03.036.
17. Lim, S. S., Vos, T., Flaxman, A. D., Danaei, G., Shibuya, K. et al. (2012). A comparative risk assessment of burden of disease and injury attributable to 67 risk factors and risk factor clusters in 21 regions, 1990–2010: A systematic analysis for the global burden of disease study 2010. *The Lancet, 380(9859),* 2224–2260. DOI 10.1016/S0140-6736(12)61766-8.
18. Angelica Hidalgo Vivas, Finn Joensen (2018). *Process and catalyst for upgrading gasoline*. US10150714B2.
19. Calcote, H. F., Manos, D. M. (1983). Effect of molecular structure on incipient soot formation. *Combustion and Flame, 49(1–3),* 289–304. DOI 10.1016/0010-2180(83)90172-4.
20. Nakakita, K., Ban, H., Takasu, S., Hotta, Y., Inagaki, K. et al. (2003). Effect of hydrocarbon molecular structure in diesel fuel on in-cylinder soot formation and exhaust emissions. *SAE International Journal of Fuels and Lubricants, 112,* 1763–1775. DOI 10.4271/2003-01-1914.
21. Schmidt, F., Reichelt, L., Päctzold, C. (2014). Catalysis of Methanol Conversion to Hydrocarbons. In: Bertau, M., Offermanns, H., Plass, L., Schmidt, F., Wernicke, H. J. (Eds.), *Methanol: The basic chemical,* pp. 423–489. Berlin Heidelberg: Springer.
22. Cang, C. D., Silvestri, A. J. (1977). The conversion of methanol and other O-compounds to hydrocarbons over zeolite catalysts. *Journal of Catalysis, 47(2),* 249–259. DOI 10.1016/0021-9517(77)90172-5.
23. Michler, T., Wippermann, N., Toedter, O., Niethammer, B., Otto, T. et al. (2020). Gasoline from the bioliq® process: Production, characterization and performance. *Fuel Processing Technology, 206,* 106476. DOI 10.1016/j.fuproc.2020.106476.
24. Stiefel, M., Ahmad, R., Arnold, U., Döring, M. (2011). Direct synthesis of dimethyl ether from carbon-monoxide-rich synthesis gas: Influence of dehydration catalysts and operating conditions. *Fuel Processing Technology, 92(8),* 1466–1474. DOI 10.1016/j.fuproc.2011.03.007.
25. Ogawa, T., Inoue, N., Shikada, T., Ohno, Y. (2003). Direct dimethyl ether synthesis. *Journal of Natural Gas Chemistry, 12,* 219–227.
26. Mao, D., Xia, J., Chen, Q., Lu, G. (2009). Highly effective conversion of syngas to dimethyl ether over the hybrid catalysts containing high-silica HMCM-22 zeolites. *Catalysis Communications, 10(5),* 620–624. DOI 10.1016/j.catcom.2008.11.003.
27. Rostrup-Nielsen, T., Højlund Nielsen, P. E., Joensen, F., Madsen, J. (2007). Polygeneration–integration of gasoline synthesis and IGCC power production using topsøe's TIGAS process. *Risoe International Energy Conference*, 56–68. Roskilde, Denmark.
28. Haro, P., Trippe, F., Stahl, R., Henrich, E. (2013). Bio-syngas to gasoline and olefins via DME–A comprehensive techno-economic assessment. *Applied Energy, 108,* 54–65. DOI 10.1016/j.apenergy.2013.03.015.
29. Dahmen, N., Dinjus, E., Kolb, T., Arnold, U., Leibold, H. et al. (2012). State of the art of the bioliq® process for synthetic biofuels production. *Environmental Progress & Sustainable Energy, 31(2),* 176–181. DOI 10.1002/ep.10624.
30. Dahmen, N., Abeln, J., Eberhard, M., Kolb, T., Leibold, H. et al. (2017). The bioliq process for producing synthetic transportation fuels. *Wiley Interdisciplinary Reviews: Energy and Environment, 6(3),* e236. DOI 10.1002/wene.236.
31. Pfitzer, C., Dahmen, N., Tröger, N., Weirich, F., Sauer, J. et al. (2016). Fast pyrolysis of wheat straw in the bioliq pilot plant. *Energy & Fuels, 30(10),* 8047–8054. DOI 10.1021/acs.energyfuels.6b01412.
32. Dahmen, N., Henrich, E., Dinjus, E., Weirich, F. (2012). The bioliq® bioslurry gasification process for the production of biosynfuels, organic chemicals, and energy. *Energy, Sustainability and Society, 2(3),* 1–44.
33. Henrich, E., Dahmen, N., Dinjus, E. (2009). Cost estimate for biosynfuel production via biosyncrude gasification. *Biofuels, Bioproducts & Biorefining, 3(1),* 28–41. DOI 10.1002/bbb.126.

34. European Parliament and the Council (1998). Directive 98/70/EC of the european parliament and of the council of 13 October 1998 relating to the quality of petrol and diesel fuels and amending council directive 93/12/EEC.
35. Weitkamp, J. (2012). Catalytic hydrocracking—Mechanisms and versatility of the process. *ChemCatChem, 4(3),* 292–306. DOI 10.1002/cctc.201100315.
36. Valavarasu, G., Bhaskar, M., Balaraman, K. S. (2003). Mild hydrocracking—A review of the process, catalysts, reactions, kinetics, and advantages. *Petroleum Science and Technology, 21(7–8),* 1185–1205. DOI 10.1081/LFT-120017883.
37. Cooper, B. H., Donnis, B. B. L. (1996). Aromatic saturation of distillates: An overview. *Applied Catalysis A: General, 137(2),* 203–223. DOI 10.1016/0926-860X(95)00258-8.
38. van den Berg, J. P., Lucien, J. P., Germaine, G., Thielemans, G. L. B. (1993). Deep desulphurisation and aromatics saturation for automotive gasoil manufacturing. *Fuel Processing Technology, 35(1–2),* 119–136. DOI 10.1016/0378-3820(93)90088-L.
39. Figueras, F., Gomez, R., Primet, M. (1973). Adsorption and catalytic properties of palladium supported by silica, alumina, magnesia, and amorphous and crystalline silica-aluminas. In: Meier, W. M., Uytterhoeven, J. B. (Eds.), *Molecular sieves*, pp. 480–489. Washington: American Chemical Society.
40. Tri, T. M., Massardier, J., Gallezot, P., Imelik, B. (1982). Additives and support effects on Pt catalysts studied by the competitive hydrogenation of benzene and toluene. *Studies in Surface Science and Catalysis, 11,* 141–148. DOI 10.1016/S0167-2991(09)61385-9.
41. Weitkamp, J. (2000). Zeolites and catalysis. *Solid State Ionics, 131(1–2),* 175–188. DOI 10.1016/S0167-2738(00)00632-9.
42. Weisz, P. B. (1980). Molecular shape selective catalysis. *Pure and Applied Chemistry, 52(9),* 2091–2103. DOI 10.1351/pac198052092091.
43. Mignard, S., Caillette, P., Marchal, N. (1993). Hydroconversion of methyl-cyclohexane on a bifunctional catalyst. In: Oballa, M. C., Shih, S. S. (Eds.), *Catalytic hydroprocessing of petroleum and disillates*, pp. 447–458. New York: CRC Press.
44. Figueras, F., Coq, B., Walter, C., Carriat, J. Y. (1997). Hydroconversion of methylcyclohexane on bifunctional sulfated zirconia-supported platinum catalysts. *Journal of Catalysis, 169(1),* 103–113. DOI 10.1006/jcat.1997.1682.
45. Weitkamp, J., Jacobs, P. A., Ernst, S. (1984). Shape selective isomerization and hydrocracking of naphthenes over Pt/Hzsm-5 zeolite. *Studies in Surface Science and Catalysis, 18,* 279–290. DOI 10.1016/S0167-2991(09)61164-2.
46. Belatel, H., Al-Kandari, H., Al-Khorafi, F., Katrib, A., Garin, F. (2004). Catalytic reactions of methyl-cyclohexane (MCH) on partially reduced moO_3. *Applied Catalysis A: General, 275(1–2),* 141–147. DOI 10.1016/j.apcata.2004.07.029.
47. Santikunaporn, M., Alvarez, W. E., Resasco, D. E. (2007). Ring contraction and selective ring opening of naphthenic molecules for octane number improvement. *Applied Catalysis A: General, 325(1),* 175–187. DOI 10.1016/j.apcata.2007.03.029.
48. Martens, G. G., Thybaut, J. W., Marin, G. B. (2001). Single-event rate parameters for the hydrocracking of cycloalkanes on Pt/US-Y zeolites. *Industrial & Engineering Chemistry Research, 40(8),* 1832–1844. DOI 10.1021/ie000799n.
49. Brouwer, D. M., Hogeveen, H. (1970). The importance of orbital orientation as a rate-controlling factor in intramolecular reactions of carbonium ions. *Recueil des Travaux Chimiques des Pays-Bas, 89(2),* 211–224. DOI 10.1002/recl.19700890213.
50. Sullivan, R. F., Egan, C. J., Langlois, G. E., Sieg, R. P. (1961). A new reaction that occurs in the hydrocracking of certain aromatic hydrocarbons. *Journal of the American Chemical Society, 83,* 1156–1160. DOI 10.1021/ja01466a036.

51. Egan, C. J., Langlois, G. E., White, R. J. (1962). Selective hydrocracking of C_9- to C_{12}-alkylcyclohexanes on acidic catalysts. evidence for the paring reaction. *Journal of the American Chemical Society, 84,* 1204–1212. DOI 10.1021/ja00866a028.
52. Santana, R. C., Do, P. T., Santikunaporn, M., Alvarez, W. E., Taylor, J. D. et al. (2006). Evaluation of different reaction strategies for the improvement of cetane number in diesel fuels. *Fuel, 85(5–6),* 643–656. DOI 10.1016/j.fuel.2005.08.028.
53. Rabl, S., Santi, D., Haas, A., Ferrari, M., Calemma, V. et al. (2011). Catalytic ring opening of decalin on Ir- and Pt-containing zeolite Y–influence of the nature of the charge-compensating alkali cations. *Microporous and Mesoporous Materials, 146(1–3),* 190–200. DOI 10.1016/j.micromeso.2011.03.045.
54. Calemma, V., Giardino, R., Ferrari, M. (2010). Upgrading of LCO by partial hydrogenation of aromatics and ring opening of naphthenes over bi-functional catalysts. *Fuel Processing Technology, 91(7),* 770–776. DOI 10.1016/j.fuproc.2010.02.012.
55. McVicker, G., Daage, M., Touvelle, M. S., Hudson, C. W., Klein, D. P. et al. (2002). Selective ring opening of naphthenic molecules. *Journal of Catalysis, 210(1),* 137–148. DOI 10.1006/jcat.2002.3685.
56. Samoila, P., Boutzeloit, M., Especel, C., Epron, F., Marécot, P. (2009). Selective ring-opening of methylcyclopentane on platinum-based bimetallic catalysts. *Applied Catalysis A: General, 369(1–2),* 104–112. DOI 10.1016/j.apcata.2009.09.006.
57. Vicerich, M. A., Benitez, V. M., Especel, C., Epron, F., Pieck, C. L. (2013). Influence of iridium content on the behavior of Pt-ir/Al_2O_3 and Pt-ir/TiO_2 catalysts for selective ring opening of naphthenes. *Applied Catalysis A: General, 453,* 167–174. DOI 10.1016/j.apcata.2012.12.015.
58. ASTM D6730 – 01 (2001). *Standard test method for determination of individual components in spark ignition engine fuels by 100-metre capillary (with precolumn) high-resolution gas chromatography*. West Conshohocken, PA: ASTM International.
59. ISO 5164 (2014). *Petroleum products-determination of knock characteristics of motor fuels-research method*. Geneva: International Organization for Standardization.
60. ISO 5163 (2014). *Petroleum products-determination of knock characteristics of motor and aviation fuels-motor method*. Geneva: International Organization for Standardization.
61. ASTM D86 (2020). *Standard test method for distillation of petroleum products and liquid fuels at atmospheric pressure*. West Conshohocken, PA: ASTM International.
62. ASTM D7345 (2017). *Standard test method for distillation of petroleum products and liquid fuels at atmospheric pressure (micro distillation method)*. West Conshohocken, PA: ASTM International.
63. ASTM D6378 (2020). *Standard test method for determination of vapor pressure (VPX) of petroleum products, hydrocarbons, and hydrocarbon-oxygenate mixtures (triple expansion method)*. West Conshohocken, PA: ASTM International.
64. Ghosh, P., Hickey, K. J., Jaffe, S. B. (2006). Development of a detailed gasoline composition-based octane model. *Industrial & Engineering Chemistry Research, 45(1),* 337–345. DOI 10.1021/ie050811h.
65. McVicker, G. B., Feeley, O. C., Ziemiak, J. J., Vaughan, D. E. W., Strohmaier, K. C. et al. (2005). Methylcyclohexane ring-contraction: A sensitive solid acidity and shape selectivity probe reaction. *The Journal of Physical Chemistry B, 109(6),* 2222–2226. DOI 10.1021/jp040205k.

Appendix A. Feed Composition for the Experiments

Table A1: Composition of the bioliq® heavy gasoline (feed)

C-Nr.	Naph.	iso-Par.	n-Par.	Cycl Ol.	Olef.	Arom.	Total
4	-	0.00	0.00	-	0.00	-	0.00
5	0.00	0.01	0.00	0.00	0.00	-	0.01
6	0.21	0.10	0.02	0.00	0.00	0.01	0.33
7	0.35	0.05	0.00	0.00	0.00	0.09	0.49
8	0.12	0.03	0.00	0.00	0.00	0.26	0.41
9	0.21	0.02	0.02	0.01	0.01	33.76	34.03
10	0.35	0.03	0.08	0.00	0.00	52.00	52.46
11	0.24	0.23	0.13	0.00	0.00	-	0.59
12 +	1.05	0.00	0.00	0.00	0.00	10.41	11.46
Poly	0.22	-	-	0.00	0.00	-	0.22
Total	2.75	0.47	0.25	0.01	0.01	96.52	100.00

Appendix B. Petrochemical Parameters of Hydroprocessed bioliq® Heavy Gasoline with Pt/HZSM-5, Pt/SAPO-11 and Pt/Mordenite

Table B1: Experimental data obtained by hydroprocessing bioliq® heavy gasoline in a fixed bed reactor under variation of the temperature

Parameters	Pt/Mordenite			Pt/HZSM-5					Pt/SAPO-11			
$T_{FB,min}$ in °C	250	270	230	250	270	290	310	330	270	310	330	350
p in bar	90	90	50	50	50	50	50	60	90	90	90	90
$WHSV$ in h^{-1}	1.39	1.39	1.39	1.39	1.39	1.39	1.39	1.39	1.39	0.88	0.88	0.88
$\dot{V}_{H_2,N}/\dot{V}_{educt}$ in–	1667	1667	1667	1667	1667	1667	1667	1667	1058	1667	1667	1667
Measurements												
$T_{FB,min}$ in °C	249.1	268.1	228.6	248.4	269.8	290.2	310.1	329.9	270.1	309.0	328.9	348.7
$T_{FB,max}$ in °C	252.8	273.3	234.3	252.8	276.2	294.7	314.9	336.8	277.9	316.0	335.4	355.1
$Y_{Gasoline}$ in wt.%	96.88	91.19	98.98	98.95	97.39	94.51	88.67	78.18	98.01	97.22	97.15	N/A
RON in–	71.6[a]	71.9[a]	N/A	71.1[a]	N/A	71.5[a]	71.8[a]	72.2[a]	N/A	N/A	N/A	N/A
MON in–	74.3[a]	75.6[a]	77.7[b]	77.3[a]	78.1[b]	78.8[a]	79.6[a]	80.8[a]	76.8[b]	77.2[b]	77.3[b]	77.3[b]
ρ in kg m^{-3}	792.7	772.0	798.6	795.7	790.7	783.0	768.0	748.0	805.6	801.7	799.8	798.4
p_v in kPa	11.0	42.0	2.3	4.8	11.9	24.0	54.0	84.0	1.4	2.8	3.8	3.8
E70 in vol.%	0.0	1.2	0.0	0.0	0.2	0.7	2.5	14.0	0.0	0.0	0.0	0.0
E100 in vol.%	0.4	6.4	0.0	0.0	0.9	3.7	10.5	23.7	0.0	0.0	0.0	0.0
E150 in vol.%	17.0	44.8	2.7	5.8	17.6	29.8	40.0	48.7	0.91	2.0	3.0	4.4
E180 in vol.%	88.5	94.1	89.2	89.9	89.7	93.5	92.5	95.3	86.9	88.7	89.2	89.3
FBP in °C	245.0	215.0	242.0	240.0	240.0	223.3	219.7	208.3	243.0	239.0	241.0	238.0
$w_{Aromatics}$ in wt.%	2.97	1.74	2.47	2.35	2.55	2.44	2.28	2.00	2.52	1.84	1.98	3.15
$w_{C10-Aromatics}$ in wt.%	0.29	0.18	0.16	0.16	0.40	0.35	0.45	0.49	0.31	0.10	0.25	0.92
$w_{iso-Par.}$ in wt.%	1.66	6.64	0.77	1.26	2.79	3.60	6.69	12.06	0.61	0.66	0.80	0.86
$w_{n-Par.}$ in wt.%	0.17	0.62	0.35	0.56	2.44	2.26	3.82	6.67	0.35	0.42	0.48	0.78

(Continued)

Table B1 (continued)

Parameters	Pt/Mordenite			Pt/HZSM-5					Pt/SAPO-11		
$w_{Naphthenes}$ in wt.%	95.17	90.96	96.39	95.84	92.19	91.64	87.16	79.22	96.51	97.08	96.70	95.16
$w_{Olefines}$ in wt.%	0.01	0.01	0.01	0.00	0.05	0.05	0.06	0.07	0	0.01	0.02	0.05

Note: a) Measured with a CFR-test engine b) Measured with FTIR according to own method.

Table B2: Experimental data obtained by hydroprocessing bioliq® heavy gasoline in a fixed bed reactor under variation of WHSV and pressure for Pt/HZSM-5

Parameters	Pt/HZSM-5									
$T_{FB,min}$ in °C	330	330	330	330	330	330	330	330	330	330
p in bar	60	60	60	60	60	70	70	70	70	70
$WHSV$ in h^{-1}	0.84	1.39	1.81	2.23	2.66	0.84	1.39	1.81	2.23	2.66
$\dot{V}_{H_2,N}/\dot{V}_{educt}$ in–	2750	1667	1279	1038	873	2750	1667	1279	1038	873
Measurements										
$T_{FB,min}$ in °C	N/A	N/A	N/A	N/A	N/A	N/A	N/A	N/A	N/A	N/A
$T_{FB,max}$ in °C	N/A	N/A	N/A	N/A	N/A	N/A	N/A	N/A	N/A	N/A
$Y_{Gasoline}$ in wt.%	67.9	65.8	81.8	87.0	88.8	60.1	72.2	74.6	88.4	88.7
RON in–	N/A	N/A	N/A	N/A	N/A	N/A	N/A	N/A	N/A	N/A
MON in–	79.5[a]	80.0[a]	79.1[a]	79.0[a]	78.5[a]	80.0[a]	N/A	N/A	78.6[a]	78.7[a]
ρ in kg m^{-3}	N/A	N/A	N/A	N/A	N/A	N/A	N/A	N/A	N/A	N/A
p_v in kPa	N/A	N/A	N/A	N/A	N/A	N/A	N/A	N/A	N/A	N/A
E70 in vol.%	28.4	18.0	11.8	12.9	2.0	23.7	N/A	N/A	7.5	9.8
E100 in vol.%	38.0	27.5	21.7	22.1	7.7	33.5	N/A	N/A	14.8	18.6
E150 in vol.%	60.3	54.4	47.0	46.4	28.0	56.1	N/A	N/A	40.0	41.7
E180 in vol.%	97.3	96.1	94.6	93.0	83.9	96.6	N/A	N/A	92.4	92.3
FBP in °C	191.7	201.8	210.8	214.5	219.4	199.6	N/A	N/A	220.8	217.7
$w_{Aromatics}$ in wt.%	1.33	0.94	1.61	4.70	8.60	1.46	0.95	1.71	3.16	4.43
$w_{C10-Aromatics}$ in wt.%	0.34	0.18	0.63	3.02	6.13	0.33	0.12	0.43	1.56	2.69
$w_{iso-Par.}$ in wt.%	20.62	14.93	11.04	9.07	7.38	19.42	13.57	11.45	8.38	7.77
$w_{n-Par.}$ in wt.%	13.63	10.75	8.72	7.44	6.15	12.58	10.05	8.66	6.68	6.28
$w_{Naphthenes}$ in wt.%	64.39	73.34	78.60	78.73	77.82	66.50	75.41	78.14	81.74	81.47
$w_{Olefines}$ in wt.%	0.04	0.03	0.04	0.05	0.06	0.05	0.04	0.04	0.05	0.05

Note: a) Measured with FTIR according to own method.

Appendix C. Petrochemical Parameters and Composition of the bioliq® Blend

Table C1: Composition of the bioliq® blend

Carbon	Naph.	iso-Par.	n-Par.	Cycl Ol.	Olef.	Arom.	Total
4	-	0.70	0.42	-	0.04	-	1.16

(Continued)

Table C1 (continued)

Carbon	Naph.	iso-Par.	n-Par.	Cycl Ol.	Olef.	Arom.	Total
5	0.11	2.12	1.20	0.00	0.09	-	3.52
6	1.44	3.88	1.28	0.03	0.15	1.15	7.94
7	2.31	1.89	0.15	0.14	0.14	12.00	16.64
8	2.92	1.21	0.08	0.33	0.14	30.93	35.61
9	8.51	0.46	0.05	0.26	0.09	11.18	20.54
10	13.85	0.36	0.02	0.09	0.05	0.02	14.38
11	0.11	0.04	0.00	0.00	0.00	-	0.14
12+	0.06	0.00	0.00	0.00	0.00	-	0.06
Poly	0.00	-	-	0.00	0.00	-	0.00
Total	29.31	10.66	3.21	0.84	0.70	55.29	100.00

Table C2: Petrochemical parameters of the bioliq® blend

Parameter	*RON*	*MON*	ρ	p_v	*E70*	*E100*	*E150*	*FBP*	$\varphi_{\text{Aromatics}}$
Unit	-	-	kg m^{-3}	kPa	vol.%	vol.%	vol.%	°C	vol.%
Value	92.4	86.2	806.22	29.7	2.5	10.4	84.4	163.2	51.4